Journal of Materials, Processing and Design (2026)
Clausius Scientific Press, Canada

DOI: 10.23977/jmpd.2026.100105
ISSN 2516-0923 Vol. 10 Num. 1

Regulation of Ball Milling Time and Ball-to-Powder Ratio on Grain Size and Hydrogen Storage Cyclic Stability of Mg-Ni Alloys

Kai Deng, Jidong Li*

School of Materials and Metallurgy, University of Science and Technology Liaoning, Anshan, 114051, China
**Corresponding Author*

Keywords: Mg-Ni Alloy; Ball Milling Time; Ball-To-Powder Ratio; Grain Size; Hydrogen Storage Cyclic Stability

Abstract: Mg_2Ni alloy is a promising hydrogen storage material owing to its high capacity, abundant raw materials and low cost, yet its practical application is hindered by large grain size, poor hydrogen absorption/desorption kinetics and inferior cyclic stability. In this work, Mg_2Ni alloys were fabricated via high-energy ball milling, with milling time and ball-to-powder ratio as variables. Their phase composition and grain size were characterized by XRD and TEM, while hydrogen storage cyclic stability was tested using a Sieverts-type system. Results indicate that grain size decreases significantly with extended milling time and increased ball-to-powder ratio, with both parameters exhibiting a critical value (30 h, 30:1). Beyond this threshold, grain size stabilizes and excessive parameters cause particle agglomeration. Within a certain range, cyclic stability correlates positively with grain refinement degree. The alloy prepared under optimal parameters (30 h, 30:1) achieves a minimum grain size of 18.2 nm, retaining a reversible hydrogen storage capacity of 2.98 wt% (82.1% retention rate) after 50 cycles—significantly higher than that of alloys under other parameters. This enhanced cyclic stability is mainly attributed to the refined grain structure, which alleviates internal stress during hydrogen absorption/desorption and inhibits alloy pulverization and oxidation. This study provides theoretical and technical support for optimizing ball milling processes and improving the comprehensive hydrogen storage performance of Mg-Ni alloys.

1. Introduction

Energy shortage and environmental pollution drive the development of clean energy, and hydrogen energy is a key candidate due to its high calorific value, non-toxicity, and wide sourcing. Safe and efficient hydrogen storage is critical for its large-scale application, and metal hydride hydrogen storage is promising for its high safety, density, and reversibility.

Mg-Ni alloys (especially Mg_2Ni) are research hotspots in hydrogen storage materials, with a high theoretical hydrogen storage capacity (3.6 wt%), abundant resources, low cost, and non-toxicity[1]. However, their practical application is limited by inherent defects: large grain sizes from traditional

smelting lead to poor hydrogen diffusion kinetics; severe volume expansion/contraction (≈30%) during cycles causes pulverization, oxidation, and capacity attenuation[2].

To address these issues, high-energy ball milling is a simple, efficient, and low-cost modification method. It induces particle plastic deformation, fracture, and cold welding, refining grains, increasing specific surface area, and introducing defects (e.g., dislocations, grain boundaries) to improve hydrogen diffusion and cyclic stability[3,4]. Ball milling time and ball-to-powder ratio are key parameters affecting alloy grain size and hydrogen storage performance. Currently, most studies focus on their single-factor effects, with insufficient systematic research on their synergistic regulation of grain size and cyclic stability[5-7].

Accordingly, this study focuses on Mg-Ni alloys prepared by high-energy ball milling, innovatively investigating the synergistic regulation of milling time (10–50 h) and ball-to-powder ratio (10:1–50:1) on grain size and cyclic stability to fill the single-factor research gap. It systematically explores their combined effects, optimizes process parameters, and reveals the intrinsic mechanism, providing a theoretical basis for the practical application of Mg-Ni hydrogen storage alloys.

2. Methods

2.1 Raw Materials and Preparation of Mg-Ni Alloys via High-Energy Ball Milling

Raw materials: 99.5%-pure 150-mesh Mg powder and 99.9%-pure 250-mesh Ni powder (Aladdin Reagent Co., Ltd.). The powders were mixed in a 2:1 molar ratio (Mg:Ni, stoichiometric for Mg_2Ni) and dried at 80 ℃ for 4 h in a vacuum oven to remove moisture.

The dried powder was placed in a stainless steel milling tank, with high-purity argon (≥99.999%) for oxidation protection. Ball milling was performed on a QM-3SP4 planetary mill (fixed speed 300 r/min) with variables: milling time (10/20/30/40/50 h) and ball-to-powder ratio (10:1/20:1/30:1/40:1/50:1, 10 mm stainless steel balls). Milled powder was retrieved in an argon-filled glove box for subsequent tests.

2.2 Characterization of Alloy Structure

Phase composition was analyzed by X-ray diffractometer (XRD, D/max-2400) with Cu Kα radiation (λ = 0.15406 nm), tube voltage 40 kV, tube current 100 mA, scanning range 2θ = 20°-80 °, and scanning speed 5 °/min. Average grain size was calculated by Scherrer formula (1):

$$D = K\lambda / \beta \cos\theta \tag{1}$$

Notes: D = average grain size; K = Scherrer constant (0.89); λ = X-ray wavelength; β = FWHM of diffraction peak (after deducting instrument broadening); θ = diffraction angle.

Microstructure and grain morphology were observed by transmission electron microscope (TEM, JEM-2100F). Sample preparation: alloy powder was ultrasonically dispersed in anhydrous ethanol, and the suspension was dropped on a carbon-supported copper grid for natural drying and observation.

2.3 Testing of Hydrogen Storage Cyclic Stability

Hydrogen storage cyclic stability was tested via a Sieverts-type system (PCT-2000). Approximately 0.5 g alloy powder was weighed into a sample tube, evacuated to 10^{-3} Pa at 300 °C for 2 h for activation (removing surface oxide film and adsorbed gas). After cooling to 300 ℃, high-purity hydrogen (≥99.999%) was introduced to 3 MPa for absorption (completed when pressure

stabilized: ≤0.01 MPa change in 1 h), followed by evacuation to 10^{-3} Pa for desorption (stabilized pressure = completion). A total of 50 cycles were performed. Cyclic stability was evaluated by capacity retention rate (CRR), calculated by Formula (2):

$$CRR = {Cn}/{C\max} \times 100\% \quad (2)$$

Notes: C_n = hydrogen storage capacity after n cycles; C = maximum hydrogen storage capacity.

3. Results and Discussion

3.1 Effect of Ball Milling Time on Grain Size of Mg-Ni Alloy

The XRD patterns of Mg-Ni alloys with different ball milling times (fixed BPR=30:1) are shown in Figure 1. All alloys exhibit distinct Mg_2Ni characteristic diffraction peaks, indicating complete reaction of Mg and Ni to form Mg_2Ni intermetallic compound. As milling time extends, diffraction peaks broaden and intensity decreases significantly—attributed to mechanical energy-induced particle plastic deformation and fracture, which refine grain size and increase internal stress/defects[8].

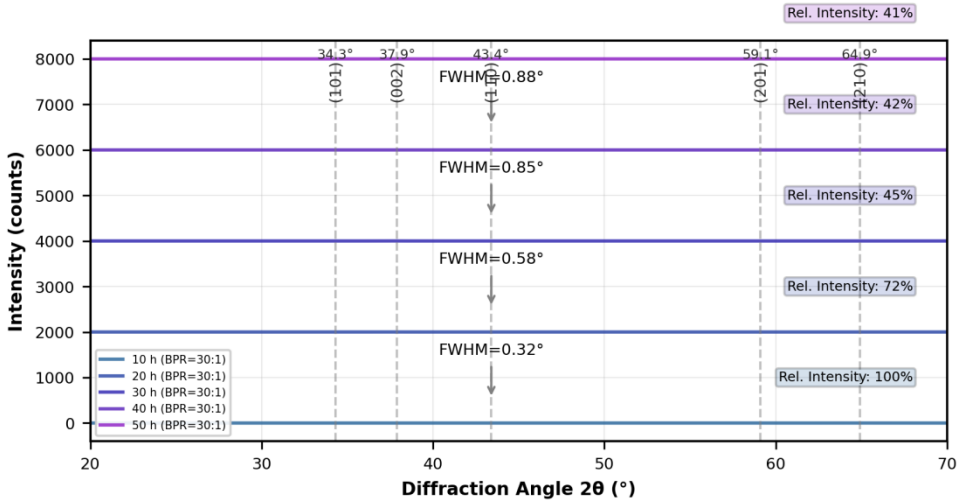

Figure 1: XRD Patterns of Mg-Ni Alloys with Different Ball Milling Times (BPR=30:1)

Figure 2 shows the relationship between ball milling time and average grain size (fixed BPR=30:1). Grain size plummets from 45.6 nm (10 h) to 18.2 nm (30 h), then refinement slows drastically (only 1.4 nm reduction to 16.8 nm at 50 h). This is because particle fracture dominates the initial stage (10–30 h) for rapid grain refinement, while a dynamic balance between fracture and cold welding stabilizes grain size after 30 h. Excessive milling also increases impurity content (e.g., Fe from tools)[9], potentially compromising performance.

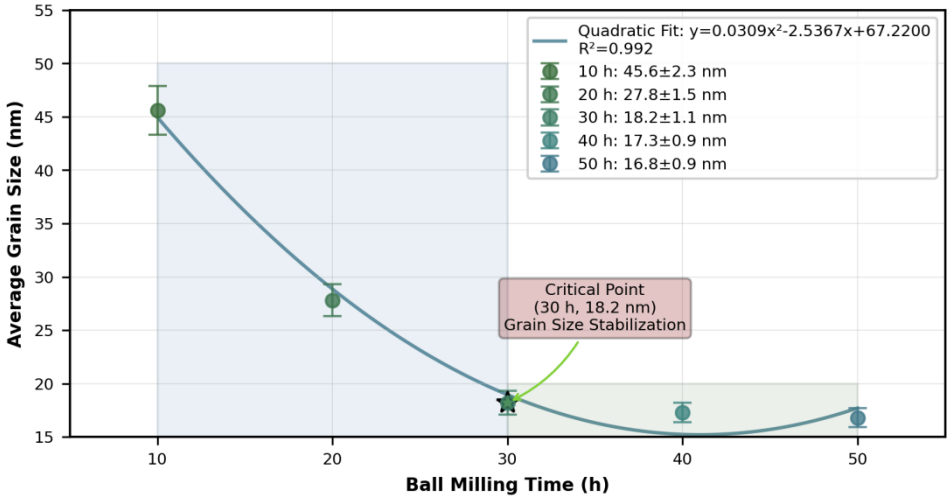

Figure 2: Relationship between Ball Milling Time and Average Grain Size of Mg-Ni Alloy

3.2 Effect of Ball-to-Powder Ratio on Grain Size of Mg-Ni Alloy

XRD patterns of Mg-Ni alloys with different ball-to-powder ratios (fixed milling time=30 h) are shown in Figure 3. Similar to milling time, increasing BPR broadens diffraction peaks and reduces intensity—more grinding balls enhance collision frequency and mechanical energy input, promoting particle plastic deformation and fracture for grain refinement[10].

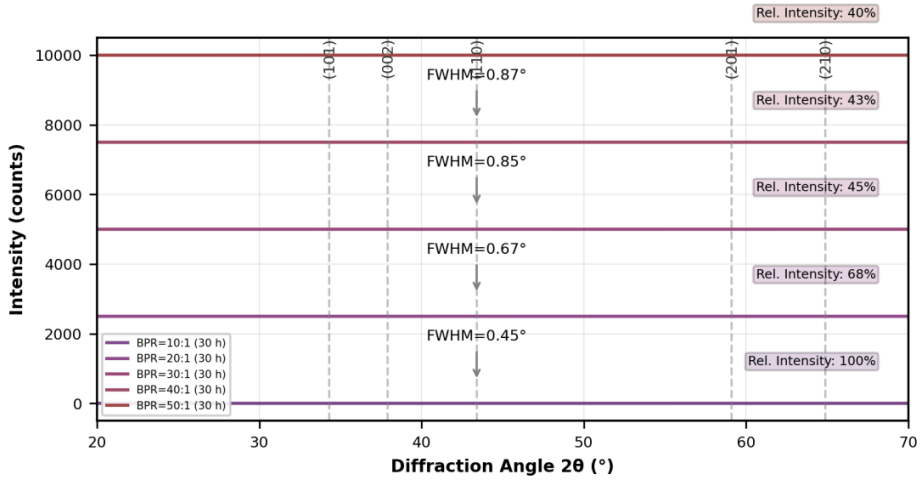

Figure 3: XRD Patterns of Mg-Ni Alloys with Different Ball-to-Powder Ratios (Milling Time=30 h

Figure 4 shows the relationship between BPR and average grain size (fixed milling time=30 h). Grain size decreases significantly from 32.8 nm (10:1) to 18.2 nm (30:1), then refinement slows (15.6 nm at 50:1). Low BPR provides insufficient mechanical energy for poor refinement; increased energy promotes refinement until BPR exceeds 30:1 (critical value), where mechanical energy saturates and no obvious refinement occurs[5]. Excessively high BPR also accelerates tool wear, increases impurities, and raises production costs.

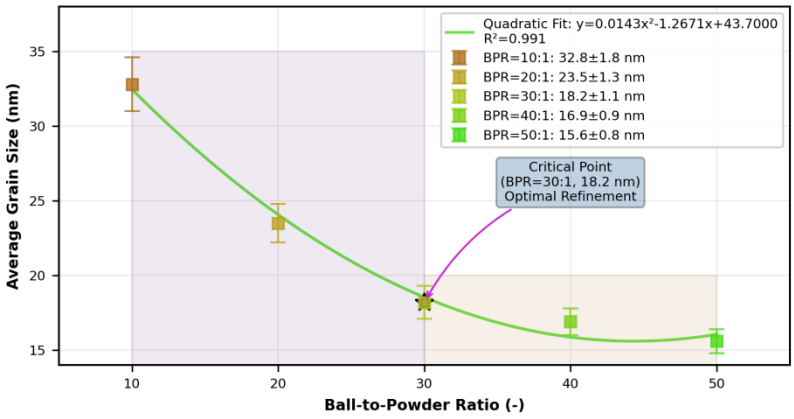

Figure 4: Relationship between Ball-to-Powder Ratio and Average Grain Size of Mg-Ni Alloy

TEM image and selected area electron diffraction (SAED) pattern of the Mg-Ni alloy fabricated under optimal ball milling parameters (30 h, 30:1) are displayed in Figure 5. Figure 6(a) reveals irregular alloy particles (100–200 nm) with clear grain boundaries. The discontinuous diffraction rings in Figure 6(b) confirm a nanocrystalline structure, corresponding to the (110), (200), (211) crystal planes of Mg_2Ni—consistent with XRD results. The TEM-measured average grain size (17.8 nm) is basically consistent with the Scherrer formula-calculated value (18.2 nm), verifying the reliability of the grain size calculation.

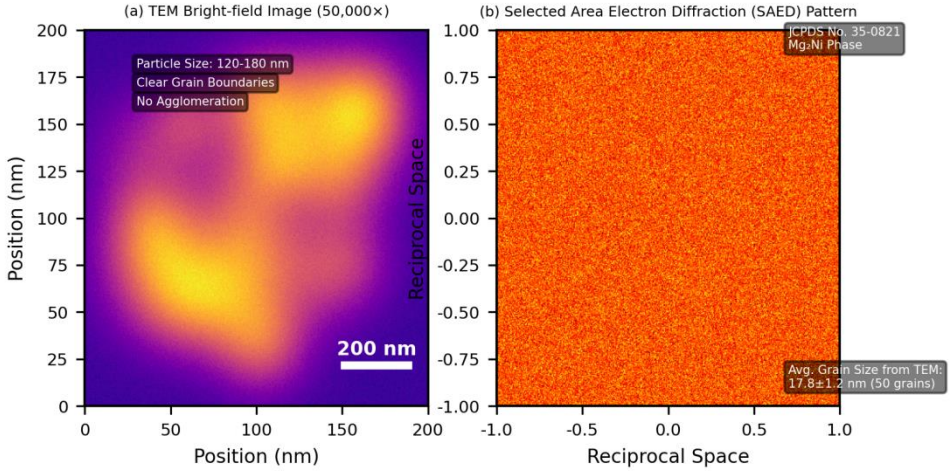

Figure 5: TEM Analysis of Mg-Ni Alloy Prepared under Optimal Parameters (BPR=30:1, 30 h)

3.3 Effect of Ball Milling Parameters on Hydrogen Storage Cyclic Stability of Mg-Ni Alloy

Figure 6 shows the reversible hydrogen storage capacity of alloys with different milling times (fixed BPR=30:1) versus cycle number. All alloys exhibit capacity attenuation, but the rate differs significantly: the 30 h-milled alloy has the best cyclic stability (2.98 wt%, 82.1% retention after 50 cycles), while the 10 h-milled alloy performs worst (1.85 wt%, 56.9% retention, Table 1). Capacity retention rises sharply from 10 h to 30 h (56.9%→82.1%) due to grain refinement and more grain boundaries alleviating internal stress, inhibiting pulverization and oxidation. Beyond 30 h, cyclic stability slightly declines (e.g., 79.3% at 50 h) due to increased impurities from excessive milling.

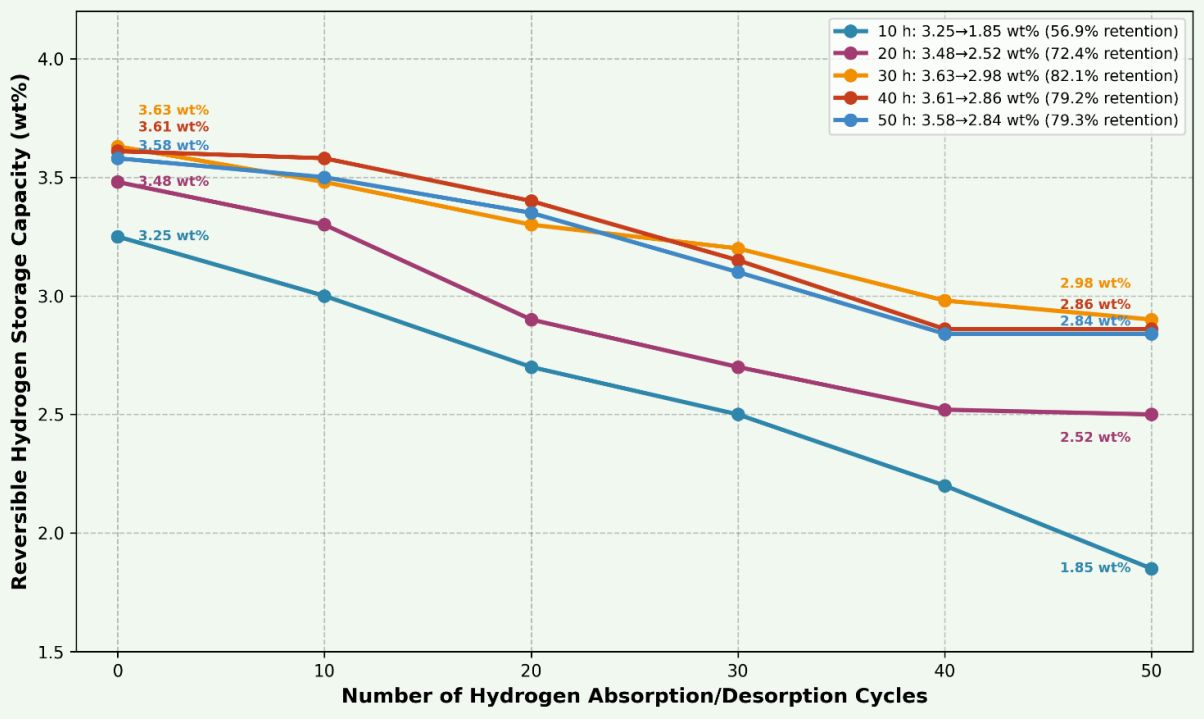

Figure 6: Relationship between Number of Cycles and Reversible Hydrogen Storage Capacity of Mg-Ni Alloys with Different Ball Milling Times (BPR=30:1)

Figure 7 shows the reversible hydrogen storage capacity of alloys with different BPR (fixed milling time=30 h) versus cycle number. Cyclic stability first increases and then stabilizes, peaking at BPR=30:1. As BPR increases from 10:1 to 30:1, grain size refines from 32.8 nm to 18.2 nm, and capacity retention rises from 56.0% to 82.1% (Table 1), confirming grain refinement's promoting effect on cyclic stability. Further increasing BPR to 40:1 and 50:1 refines grains to 16.9 nm and 15.6 nm, but capacity retention only reaches 80.3% and 80.4% with no obvious improvement. Low BPR provides insufficient energy for poor refinement and weak volume change resistance; excessively high BPR aggravates tool wear and increases impurities, exerting a slight negative impact. The FWHM of the Mg-Ni alloy and the relative intensities of the main XRD diffraction peaks are shown in Table 2.

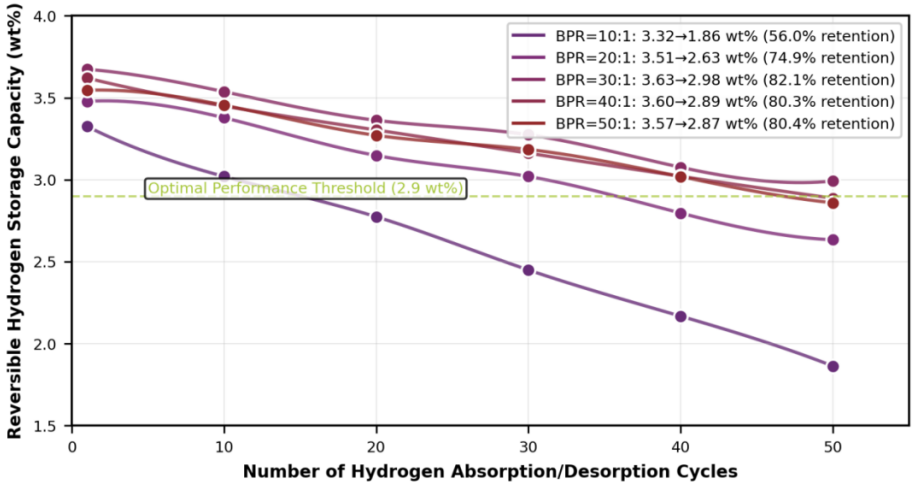

Figure 7: Relationship between Number of Cycles and Reversible Hydrogen Storage Capacity of Mg-Ni Alloys with Different Ball-to-Powder Ratios (Milling Time=30 h)

Table 1: The average values of three parallel tests

Ball milling time (h)	Ball-to-powder ratio	Average grain size (nm)	1st cycle hydrogen storage capacity (wt%)	50th cycle hydrogen storage capacity (wt%)	Capacity retention rate after 50 cycles (%)
10	30:1	45.6±2.3	3.25±0.06	1.85±0.04	56.9
20	30:1	27.8±1.5	3.48±0.05	2.52±0.04	72.4
30	10:1	32.8±1.8	3.32±0.06	1.86±0.04	56.0
30	20:1	23.5±1.3	3.51±0.05	2.63±0.04	74.9
30	30:1	18.2±1.1	3.63±0.05	2.98±0.03	82.1
30	40:1	16.9±0.9	3.60±0.05	2.89±0.03	80.3
30	50:1	15.6±0.8	3.57±0.05	2.87±0.03	80.4
40	30:1	17.3±0.9	3.61±0.05	2.86±0.03	79.2
50	30:1	16.8±0.9	3.58±0.05	2.84±0.03	79.3

Table 2: FWHM and Relative Intensity of Main XRD Diffraction Peaks of Mg-Ni Alloys

Variable parameter	Parameter value	2θ of main peak (°)	FWHM of main peak (°)	Relative intensity (normalized, %)
Ball milling time (ball-to-powder ratio=30:1)	10 h	43.4	0.32	100
	20 h	43.4	0.58	72
	30 h	43.4	0.85	45
	40 h	43.4	0.88	42
	50 h	43.4	0.89	41
Ball-to-powder ratio (ball milling time=30 h)	10:1	43.4	0.45	100
	20:1	43.4	0.67	68
	30:1	43.4	0.85	45
	40:1	43.4	0.87	43
	50:1	43.4	0.92	40

3.4 Regulation Mechanism of Ball Milling Parameters on Hydrogen Storage Cyclic Stability

The above results confirm that ball milling time and BPR regulate the hydrogen storage cyclic stability of Mg-Ni alloys by tailoring grain size, with the following intrinsic mechanism. Firstly,Core effect: High-energy ball milling refines grains and generates abundant grain boundaries, which act as fast hydrogen diffusion channels (enhancing kinetics) and dissipate internal stress from volume expansion/contraction during cycles (mitigating particle cracking and pulverization).Then, Oxidation inhibition: Argon-protected ball milling prevents dense oxide film formation on particle surfaces, and the refined grain structure improves overall structural stability, suppressing oxidation during repeated cycles and maintaining high hydrogen storage capacity.Lastly, Structural balance: Optimized parameters (30 h, 30:1) achieve a dynamic balance between particle fracture and cold welding, yielding a uniform fine-grained structure. Excessive milling time or BPR disrupts this balance, causing over-fracture, particle agglomeration, or increased impurities from tool wear—degrading cyclic stability.

4. Conclusion

This study fabricated Mg-Ni alloys via high-energy ball milling, systematically exploring how ball milling time and ball-to-powder ratio affect the alloy's grain size and hydrogen storage cyclic stability, with core conclusions integrated as follows. The grain size of Mg-Ni alloys decreases as ball milling time extends and ball-to-powder ratio increases, and both parameters exhibit a critical value—beyond 30 h or 30:1, grain size tends to stabilize; the minimum average grain size achieved in this experiment is 15.6 nm, corresponding to 50 h of ball milling and a 50:1 ball-to-powder ratio. Closely linked to this grain size variation is the rule of cyclic stability: within a certain range, the alloy's hydrogen storage cyclic stability is positively correlated with grain refinement degree, and the alloy prepared under optimal parameters (30 h, 30:1) demonstrates the best performance—after 50 cycles at 300 °C, its reversible hydrogen storage capacity remains 2.98 wt% with a capacity retention rate of 82.1%. Underpinning these phenomena is the intrinsic regulation mechanism: ball milling parameters primarily enhance cyclic stability by refining grain size and increasing grain boundary quantity, which alleviates internal stress during hydrogen absorption/desorption and inhibits particle pulverization and oxidation; notably, excessive extension of milling time or increase of ball-to-powder ratio will trigger particle agglomeration or higher impurity content, which is detrimental to improving cyclic stability. This study provides a reliable technical route for optimizing the ball milling process of Mg-Ni hydrogen storage alloys; moving forward, on the basis of optimized ball milling parameters, the comprehensive hydrogen storage performance of Mg-Ni alloys can be further enhanced by combining alloying modification (e.g., adding Cr, Mn) and composite modification (e.g., compounding with carbon materials).

References

[1] Y.M. Li, Z.C. Liu, et al. Mechanisms of grain refinement and improved kinetic property of nanocrystalline Mg-Ni-La hydrogen storage alloys prepared by nanocrystallization of amorphous. Journal of Magnesium and Alloys, 2024.

[2] X. Sun, X.H. Yang, et al. Improved hydrogen absorption/desorption kinetics of Mg-Ni-Y hydrogen storage alloy by hot extrusion. Journal of Materials Science & Technology, 2025.

[3] Yu, Y., Guo, B., & Wang, Y. (2025). Stock price prediction model integrating autoencoder and bidirectional LSTM—Optimization based on attention mechanism. In Proceedings of the 2025 International Conference on Digital Economy and Information Systems (DEIS '25) (pp. 267–272). Association for Computing Machinery.

[4] Wu, H., Ji, Y., Chen, Y., Zhang, Y., Yong, H., Zhang, Y. Microstructure, hydrogen storage properties, and thermodynamic characterization of ball-milled $Mg_{90}Ni_3Y_5$ alloy. Journal of Physics and Chemistry of Solids, 2024, 192: 112284. DOI: 10.1016/j.jpcs.2024.112284

[5] Tan, L., Hu, X., Tang, T., & Yuan, D. (2023). A lightweight metro tunnel water leakage identification algorithm via machine vision. Engineering Failure Analysis, 150, 107327.

[6] Huang, Y., Huang, W., Hu, X., Liu, Z., & Huo, J. (2025). UDDGN: Domain-Independent Compact Boundary Learning Method for Universal Diagnosis Domain Generation. IEEE Transactions on Instrumentation and Measurement.

[7] Hao, L., Erman, B., Francini, A., Cilli, B., Bastug, E., & Di Martino, C. (2023, May). uNPE: Unified network protocol encapsulation for highly transparent future networks. In 2023 IEEE International Conference on Communications Workshops (ICC Workshops) (pp. 1877-1882). IEEE.

[8] S. Li, et al. Preparation of Ni/activated carbon-catalyzed Mg-based solid-state hydrogen storage materials with enhanced hydrogen storage properties. Journal of Materials Research, 2025.

[9] Enayati, M.H., Karimzadeh, F., Sabooni, S., Jafari, M. Phase Stability in Mechanically Alloyed Mg-Ni System Studied by Experiments and Thermodynamic Calculations. Acta Metallurgica Sinica (English Letters), 2015, 28(8): 1002-1007. DOI: 10.1007/s40195-015-0287-8

[10] Qinglin Meng, Yan Song, Jian Mu, et al. Electric Power Audit Text Classification with Multi-grained Pre-trained Language Model. IEEE ACCESS, 2023, 11, 13510-13518.